Thermal Conductivity of Fluids. Nitrogen Dioxide in the Liquid Phase

G. N. RICHTER AND B. H. SAGE
California Institute of Technology, Pasadena, Calif.

Thermal conductivity of fluids is a transport characteristic useful in predicting thermal transfer. The background of experimental data in this field is not extensive even for many fluids of industrial importance. A recent review by Keyes (*7*) is an excellent summary of the data available for a number of gases. Measurements for nitrogen, carbon dioxide, and their mixtures are available (*8*). The thermal conductivity and some other properties for 11 gases were also reported by Keyes (*10*). Andrussow studied the thermal conductivity of hydrogen, deuterium, helium, neon, and their mixtures (*1*). Comings and coworkers made a number of measurements of the thermal conductivity of nitrogen, methane, ethane, and argon at elevated pressures and presented a correlation to permit the prediction of this transport property (*12*).

Sellschopp (*22*) and Vargaftik (*24*) studied the thermal conductivity of gases at high pressures. Filippov contributed some measurements of thermal conductivity involving the use of the plane-layer technique (*3*). Mason reported the thermal conductivity of some 20 liquids of industrial importance at temperatures between 32° and 212° F. (*13*). This transport property for steam and nitrogen was reported by Keyes and Sandell (*11*). Kannuluik and Martin (*6*) measured the thermal conductivity of helium at 32° F. The behavior of helium was reported also by Ubbink and de Haas (*23*). Sakiadis and Coates (*20*) have prepared a useful critical summary of the thermal conductivity of liquids which has been correlated upon the basis of the theorem of corresponding states. Rothman and Bromley (*18*) studied the thermal conductivity of nitrogen, carbon dioxide, argon, and mixtures of nitrogen and carbon dioxide to a maximum temperature of about 1400° F.

Keyes reported the thermal conductivity of nitrous oxide (*10*) at pressures up to 2100 pounds per square inch; and Johnston and Grilly (*5*) studied nitric oxide. However, data appear to be lacking concerning the thermal conductivity of other oxides of nitrogen or their mixtures. For this reason measurements of the thermal conductivity of nitrogen dioxide in the liquid phase were undertaken. These studies were made at pressures up to 5000 pounds per square inch in the temperature interval between 40° and 160° F.

METHODS OF MEASUREMENT

Many types of equipment have been employed for the determination of the thermal conductivity of fluids. Keyes (*9*) described in detail equipment used for measurements of this property. Many of these investigations were made with equipment utilizing an internal cylindrical heating element and an external cylinder maintained at a constant but lower temperature. In the case of apparatus to be operated at high pressures it is necessary to avoid deformation of the solid boundaries of the system as a result of the forces involved. In addition, many measurements (*3*) were made using the space between parallel plates as the transport path.

In the interest of avoiding thermal leakage around the peripheries of plane surfaces or at the ends of the cylindrical section, a spherical configuration was employed in this investigation. A schematic arrangement of the conductivity equipment is shown in Figure 1. In principle, it consists of vessel *A* which is immersed in an agitated liquid bath, *B*, maintained at a constant temperature. Interior sphere *C* is provided with an electric heater, *D*, which permits the sphere to be maintained above the temperature of the surroundings. Energy addition through the electric heater is determined by conventional calorimetric techniques. Interior sphere *C* is surrounded by two carefully machined spherical shells *E* and *F*. Thermocouples were mounted in the shells near the internal face of shell *E* and the external face of shell *F*. Dimensions of these spherical shells are known with accuracy and since they are pressure-compensated, it is possible to determine the spacing between them as functions of pressure and temperature.

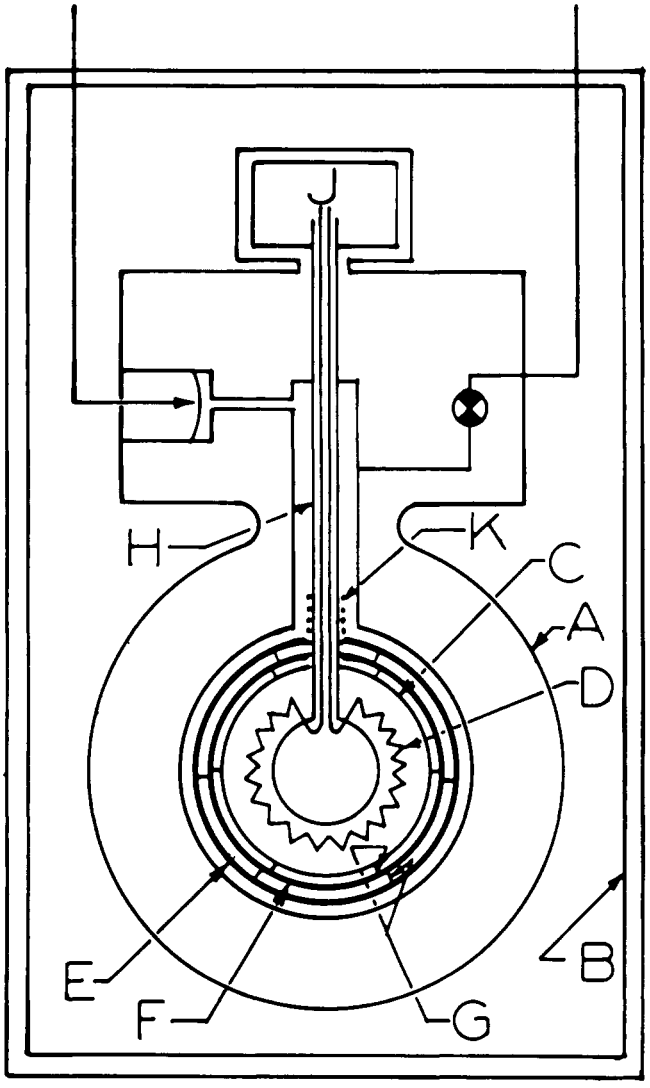

Figure 1. Arrangement of conductivity cell

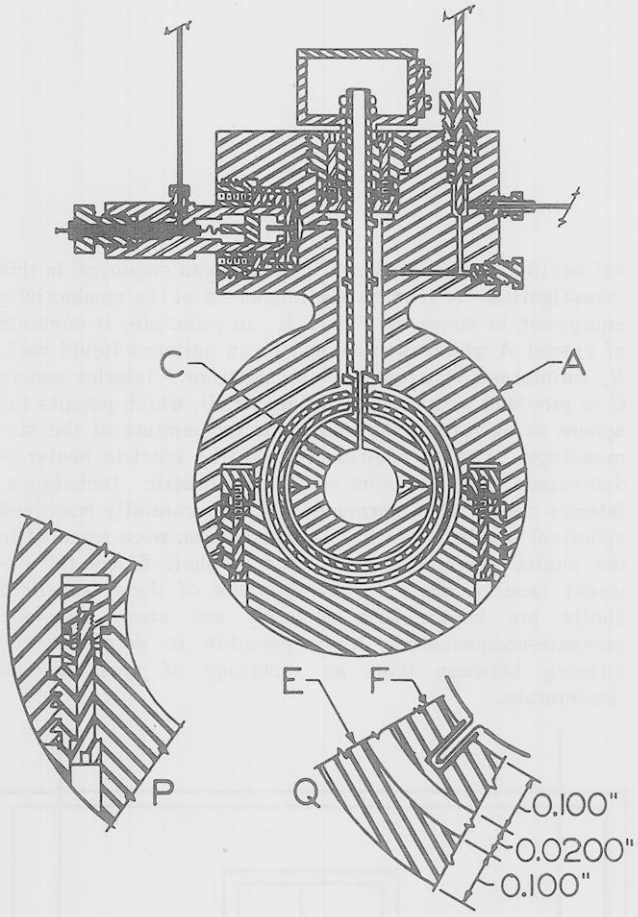

Figure 2. Sectional view of conductivity cell

The shells were spaced by six pins shown at *G* in Figure 1. The pins were constructed of low thermal conductivity steel and, at each point of contact with the adjacent sphere, were less than 0.010 inch in diameter. From a knowledge of the energy addition through heater *D* and the differences in temperature between the inner surface of *E* and the outer surface of *F*, it was possible in principle to obtain the thermal conductivity from the following equation (*4*):

$$k = \frac{\mathring{q}_m (r_o - r_i)}{4\pi r_o r_i (T_i - T_o)} \qquad (1)$$

Equation 1 neglects the area associated with stem *H* containing leads *J* (Figure 1). It also assumes that all the energy transport occurs by conduction through the spherical shell of fluid. Corrections for this small difference in area, which amounted to less than 0.22%, along with those for radiation and gains or losses by conduction through stem *H* and supporting pins *G*, may be incorporated in Equation 1 to yield

$$k = \left[\frac{(\mathring{q}_m - \mathring{q}_r - \mathring{q}_s - \mathring{q}_p)(r_o - r_i)}{4\pi r_o r_i (T_i - T_o)}\right] \phi_A \qquad (2)$$

In the derivation of Equation 2, the area of the stem corresponding to the average of the inner radius of *E* and the outer radius of *F* was employed. The radiation corrections were determined by measurements with the interior of the conductivity cell evacuated to a pressure less than 10^{-6} inch of mercury. In the case of investigations with nitrogen dioxide the optical absorbance was great enough to render this effect negligible.

The term accounting for thermal leakage in stem *H* was established by measuring the temperature gradient in the vicinity of the guard heater, *K*, with a differential thermocouple. It was found that the total corrections for losses through the stem could be kept less than 0.0001 of the energy added to heater *D*. Losses through supporting pins *G* were calculated from their dimensions and the measured temperature difference between shells *E* and *F*. The maximum correction on this account was 0.0060 of the energy added.

In measuring thermal conductivity in a configuration such as shown in Figure 1 it was necessary to eliminate natural convection from the reported value of thermal conductivity. Natural convection should be negligible when the product of the Prandtl and Grashof numbers is less than 1000 (*11*). With a clearance of 0.020 inch, which was used in this equipment, the maximum temperature difference between the inner surface of *E* and the outer surface of *F* was varied between 2° and 4°F. depending upon the volumetric properties of the nitrogen dioxide. To establish the Grashof number for these conditions, available volumetric and viscosity measurements of nitrogen dioxide were employed (*15, 16, 21*). It was found that there was limited variation in the value of thermal conductivity as determined from Equation 2 with the temperature difference employed, even for situations where the product of the Prandtl and Grashof numbers was markedly less than 1000. As a result of this variation, data were obtained at several different temperature gradients and the apparent thermal conductivity was extrapolated to zero temperature difference to obtain the reported value of thermal conductivity.

EQUIPMENT

A sectional view of the conductivity cell is shown in Figure 2. The apparatus was constructed of a stainless steel pressure vessel, *A*, containing 25 weight % of chromium and 20 weight % of nickel. Insert *P* of Figure 2 shows the closure of the pressure vessel. Figure 3 is a photograph of one of the concentric spheres before assembly. These hemispheres, shown at *E* and *F* in Figures 1 and 2, were machined to a spherical surface within a maximum deviation of 0.0005 and an average deviation of 0.0002 inch. The effective path length between the inner surface of *E* and the outer surface of *F*, shown in insert *Q* of Figure 2, was determined by filling the space with mercury and determining the gain in weight of the system. From the measurements with mercury an average difference in radius of 0.01997 inch was found at 74°F. between the inner surface of *E* and the outer surface of *F*. From the dimensions of the spheres a separation of 0.0200 inch was

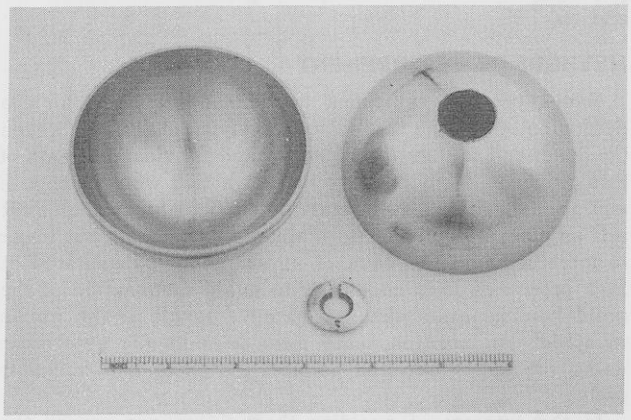

Figure 3. Appearance of concentric spheres

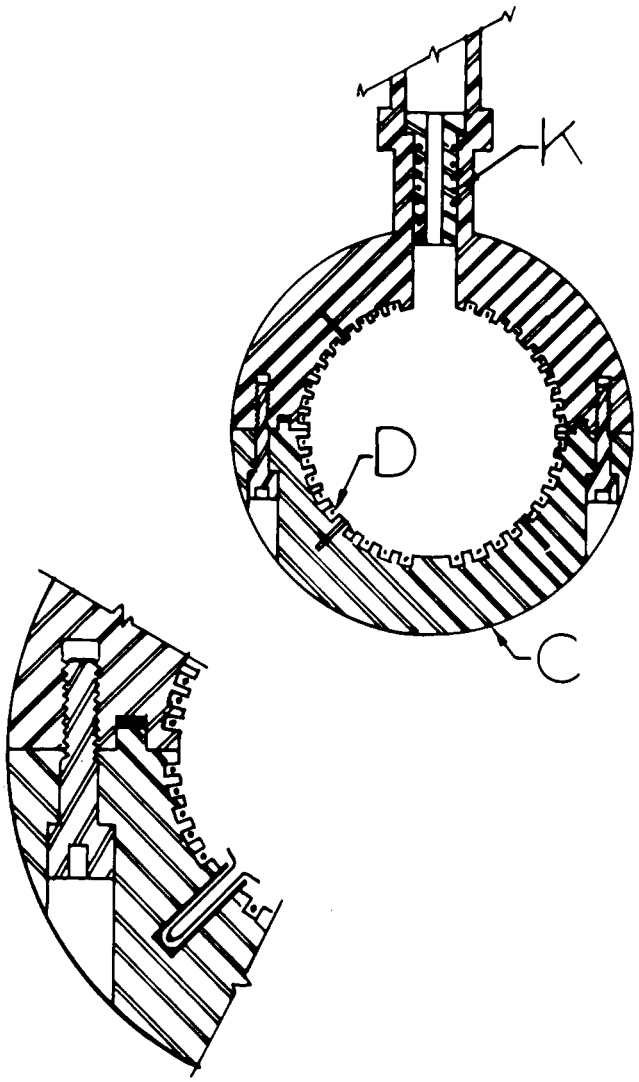

Figure 4. Details of construction of heated sphere

obtained. The value determined with mercury was used as the basis for calculations of thermal conductivity. The change in radius with temperature and pressure was calculated from known values of thermal expansion and elastic properties of steel. The change in dimensions with pressure for the shells was found to be negligible over the range of conditions encountered in the present study but might be significant for measurements at much higher pressures.

Four-junction platinum, platinum-iridium thermocouples were used for the measurements of the difference in temperature between the surfaces of *E* and *F*. One such thermocouple was located in the upper half of the shells and one in the lower half. The thermocouples were constructed of wire 0.003 inch in diameter and were provided with glass insulation. In order to avoid uncertainty from temperature gradients in the wire, the leads to the thermocouples were mounted in close-fitting wells in the thin shells as shown in insert *Q* of Figure 2. The thermocouples were mounted within 0.015 inch of the inner surface of *E* and the outer surface of *F*. Glass insulation 0.002 inch thick was employed around each thermocouple. Four copper-constantan thermocouples were used to determine the difference in temperature of sphere *C* and sphere *A*.

A differential thermocouple of the latter type was also used to determine the gradient in stem *H* near the guard heater, *K*, of Figure 1. This heater was wound upon a small metal spool and soldered with lead to the interior of stem *H*. The details of the guard heater *K* and the primary heater *D*, along with the unsupported area seal used as the closure of the inner sphere *C*, are shown in Figure 4.

The thermocouples were standardized by comparison with a strain-free platinum resistance thermometer which had been calibrated by the National Bureau of Standards. Electromotive force measurements of the differential thermocouple were made with a White-type double potentiometer. An uncertainty of 0.1 microvolt, corresponding to a maximum temperature difference between the shells of 0.008°F., was involved in the determinations.

The conductivity cell, *A*, was placed within an agitated bath *B* of conventional design (Figure 5). Agitation was provided by means of the impeller, *L*, which was driven through a packing gland located at the bottom of the bath. A radiation shield, *M*, which could be heated or cooled was provided in order to avoid the need for adding more than 100 watts of power to the internal heater of the bath. The energy added to the internal heater was controlled by a modulating circuit which has been described (*17*). Explorations with a resistance thermometer indicated that the variation in temperature with space and time in the bath was less than 0.01°F. At a given point variations with time were less than 0.006°F. The temperature of the bath was determined from the indications of a strain-free platinum resistance thermometer of the coil filament type (*14*) which had been compared with a similar instrument cali-

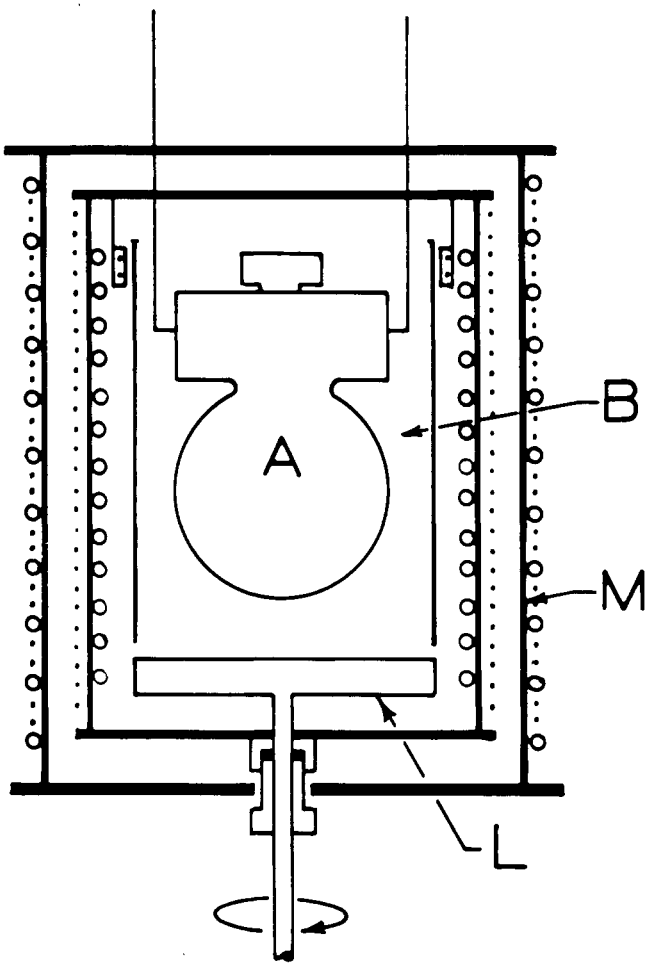

Figure 5. General arrangement of equipment

brated by the National Bureau of Standards. It is believed that the temperature of the bath was known within 0.01 °F. relative to the international platinum scale throughout the range of temperatures between 40° and 400 °F.

Pressure in the conductivity cell was measured by means of a balance (*19*) which was calibrated against the vapor pressure of carbon dioxide at the ice point (*2*). The balance was connected to the conductivity cell through a diaphragm of the aneroid type (*21*). Pressures within the cell were known within 0.3 pound per square inch or 0.1%, whichever was the larger measure of uncertainty. The nitrogen dioxide was introduced into the thermal conductivity cell at low temperatures and the requisite pressure within the vessel was obtained by raising the temperature. Measurements were made for at least three different temperature differentials at each state.

HEAT LOSSES

By regulation of guard heater *K*, Figure 1, the thermal losses through stem *H* were made negligibly small. From a knowledge of the dimensions of the stem and the physical properties of the materials, the actual leakage could be calculated on the basis of the observed temperature gradient. The instantaneous thermal flux as a function of time for two typical sets of measurement is shown in Figure 6, and in all cases was less than 0.0001 of the energy added to heater *D*. The magnitude of the thermal transfer was checked by measuring the change in temperature of sphere *C*, shown in Figure 1, at constant energy input with changes in the temperature gradient in the stem.

Thermal flux in supporting pins *G* was minimized by making them small. A solution of the heat transfer equation for the pins yields an expression of the following form:

$$\mathring{q}_p = \frac{24 r_p^2 \pi k_{st} (T_i - T_o)}{5 (r_o - r_i)} \qquad (3)$$

After substitution of the appropriate dimensional numerical constants obtained from calibration of the thermal losses, Equation 3 simplifies to

$$\mathring{q}_p = \frac{2\pi k_{st} (T_i - T_o)}{1000} \qquad (4)$$

The thermal flux was between 0.0043 and 0.0060 of the power added to sphere *C* of Figure 1. The pins were approximately 0.01 inch in diameter but their effective dimensions for thermal transport were determined by direct calibration. Corrections for these effects were made as was indicated in Equation 2. Because of their small size, even relatively large errors in estimating these fluxes would exert only a small effect on the calculated thermal conductivities.

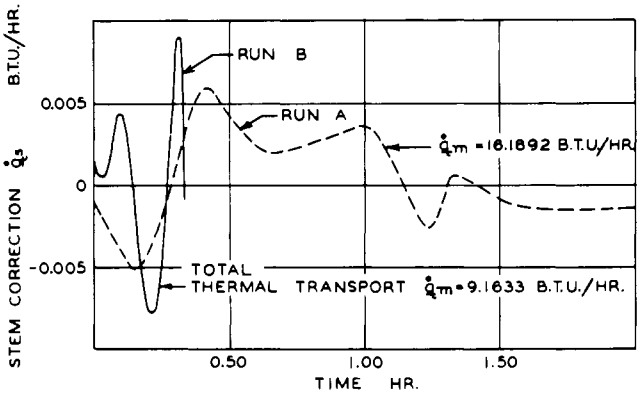

Figure 6. Thermal flux as function of time

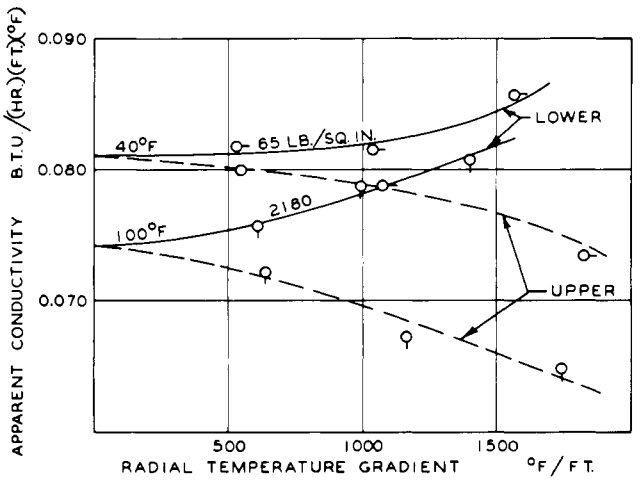

Figure 7. Influence of temperature gradient upon apparent thermal conductivity

MATERIALS

The nitrogen dioxide employed in this investigation was obtained from The Matheson Co., Inc., which reported it to contain 0.02 weight fraction of impurities. The sample was fractionated in a glass column containing 30 glass plates at a reflux ratio of approximately 5. The first and last 15% of the overhead were discarded. The central portion of the overhead from the fractionation was dried over phosphorus pentoxide and collected at the temperature of liquid nitrogen. The purified sample was stored in a stainless steel container until it was introduced into the thermal conductivity cell. It appears that this material contained less than 0.002 mole fraction of material other than nitrogen dioxide.

EXPERIMENTAL RESULTS

The dimensional constants of the equipment are given in Table I. The results of a series of measurements at 40° and 100 °F. are shown in Figure 7 and are recorded in Table II. The variation in the apparent thermal conductivity with temperature difference between the shells is significant but yet not great enough to cause uncertainty in the limiting value corresponding to zero temperature difference. The differing behavior in the upper and lower hemispheres may well result from limited local circulation in the upper hemisphere, since the temperature gradients with respect to the gravitational field are reversed in the two hemispheres. These differences in behavior between the thermocouples located in the lower and upper hemispheres are evident. Table II also includes details of the experimental data in order that they may be re-evaluated if desired.

Table I. Pertinent Dimensions of Equipment

Quantity[a]	Units	Temperature, °F.		
		40	100	160
$(r_o - r_i)$	Feet	1.6639×10^{-3}	1.6647×10^{-3}	1.6655×10^{-3}
$\left(\frac{r_o - r_i}{4\pi r_i r_o}\right)$	$Feet^{-1}$	6.7958×10^{-3}	6.7926×10^{-3}	6.7893×10^{-3}
ϕ_A		1.00218	1.00218	1.00218

[a] See nomenclature.

A summary of the experimental values of thermal conductivity obtained is presented in Table III as a tabular function of pressure for each temperature. The effect of

Table II. Sample Experimental Thermal Conductivity Measurements

Quantity	Symbol	Units	Conditions					
Bath temperature	T	°F.	40	40	40	100	100	100
Pressure at zero flux	P	Lb./sq.in.abs.	65.0	65.0	65.0	2179.8	2179.8	2179.8
Measured energy input rate	$\dot{q}_m$	B.t.u./hr.	10.6667	20.7281	32.7949	11.3104	19.2069	27.6692
Pressure	P	Lb./sq.in.abs.	315.6	529.5	766.7	2414.2	2559.0	2705.1
Upper half sphere								
Temperature difference	$(T_i - T_o)$	°F.	0.905	1.786	3.034	1.062	1.937	2.898
Rate of loss through pins	$\dot{q}_p$	B.t.u./hr.	0.0415	0.0819	0.1392	0.0507	0.0925	0.1384
Transfer by conduction	$\dot{q}_c$	B.t.u./hr.	10.6471	20.6898	32.7256	11.2833	19.1551	27.5899
Apparent thermal conductivity	k_{app}	B.t.u./(hr.)(ft.)(°F.)	0.0780	0.0787	0.0733	0.0722	0.0672	0.0647
Lower half sphere								
Temperature difference	$(T_i - T_o)$	°F.	0.884	1.726	2.597	1.014	1.656	2.324
Rate of loss through pins	$\dot{q}_p$	B.t.u./hr.	0.0405	0.0792	0.1191	0.0484	0.0791	0.1110
Transfer by conduction	$\dot{q}_c$	B.t.u./hr.	10.6496	20.6941	32.7472	11.2860	19.1690	27.6177
Apparent thermal conductivity	k_{app}	B.t.u./(hr.)(ft.)(°F.)	0.0818	0.0815	0.0857	0.0756	0.0786	0.0807
Thermal conductivity[a]	k	B.t.u./(hr.)(ft.)(°F.)	0.0811	0.0811	0.0811	0.0742	0.0742	0.0742

[a]Extrapolated to zero flux.

pressure upon thermal conductivity in the liquid phase constitutes Figure 8. The experimental points depicted in Figure 8 yield a standard deviation of 0.00058 B.t.u. per hour-foot-°F. from the smooth curves.

Thermal conductivities for even values of pressure and temperature are recorded in Table IV for nitrogen dioxide. From the measurements of electrical energy addition, temperature differences, and thermal losses it appears that the probable error in the reported values of thermal conductivity is 0.0015 B.t.u. per hour-foot-°F.

Deterioration of the thermocouples and other parts of the equipment as a result of attempts to make investigations at higher temperatures than those reported here prevented a desirable check upon the over-all accuracy of the equipment by measurements upon a gas with known thermal conductivities, such as nitrogen. After reassembly such comparisons were made and satisfactory agreement was obtained, but such data are not directly relevant to this investigation.

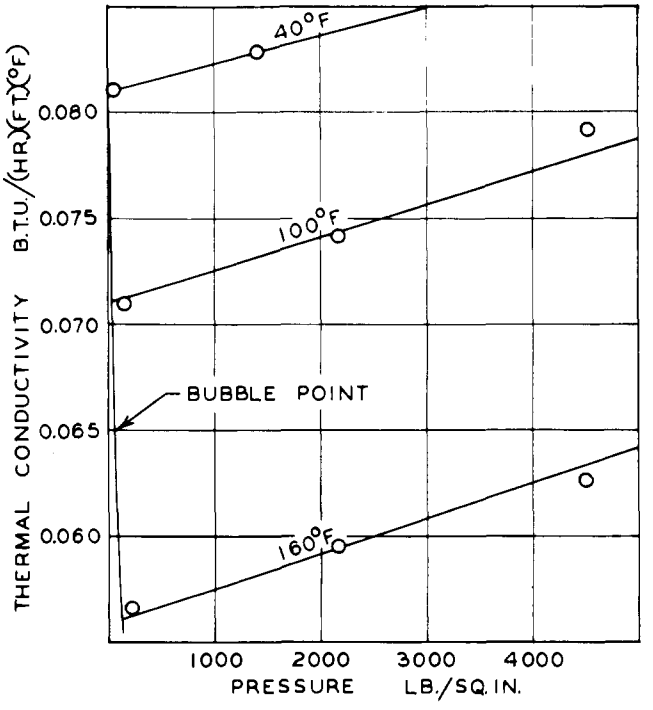

Figure 8. Thermal conductivity of nitrogen dioxide in liquid phase

Table III. Experimental Values of Thermal Conductivity of Nitrogen Dioxide in Liquid Phase

Temp., °F.	Pressure, Lb./Sq. Inch Absolute	Thermal Conductivity, B.t.u./(Hr.)(Ft.)(°F.)
40	65.0	0.0811
	1418.	0.0827
100	157.9	0.0710
	2179.8	0.0742
	4522.0	0.0791
160	219.3	0.0566
	2167.7	0.0596
	4517.5	0.0626

Table IV. Thermal Conductivity of Nitrogen Dioxide in Liquid Phase

Pressure, Lb./Sq. Inch Absolute	40°F. (6.6)[a,b]	100°F. (30.7)	160°F. (111.2)
Bubble point	0.0809[c]	0.0715	0.0560
200	0.0812	0.0717	0.0562
400	0.0815	0.0720	0.0565
600	0.0817	0.0723	0.0568
800	0.0820	0.0726	0.0572
1000	0.0823	0.0729	0.0575
1250	0.0826	0.0733	0.0579
1500	0.0829	0.0736	0.0584
1750	0.0833	0.0740	0.0588
2000	0.0836	0.0744	0.0592
2250	0.0839	0.0747	0.0596
2500	0.0843	0.0751	0.0600
2750	0.0846	0.0754	0.0604
3000	0.0849	0.0758	0.0609
3500	...	0.0765	0.0617
4000	...	0.0772	0.0625
4500	...	0.0780	0.0634
5000	...	0.0787	0.0642

[a] Values in parentheses represent bubble-point pressures expressed in pounds per square inch absolute.
[b] Bubble-point pressure at 40°F. extrapolated.
[c] Thermal conductivity expressed in B.t.u./(hr.)(ft.)(°F.).

NOMENCLATURE

k = thermal conductivity
k_{st} = thermal conductivity of steel
$\dot{q}_c$ = rate of transfer by conduction through fluid
$\dot{q}_m$ = measured energy input rate
$\dot{q}_p$ = rate of loss through supporting pins
$\dot{q}_r$ = rate of transfer by radiation
$\dot{q}_s$ = rate of loss up stem
r_i = inner radius
r_o = outer radius
r_p = radius of supporting pins

T_i = temperature at inner boundary
T_o = temperature at outer boundary
ϕ_A = ratio of area of complete sphere to that of sphere minus area intersected by stem

ACKNOWLEDGMENT

W. M. DeWitt constructed the thermal conductivity cell, H. H. Reamer aided materially in obtaining the experimental results, and W. N. Lacey reviewed the manuscript.

LITERATURE CITED

(1) Andrussow, L., *J. chim phys.* **49**, 599 (1952).
(2) Bridgeman, O. C., *J. Am. Chem. Soc.* **49**, 1174 (1927).
(3) Filippov, L. P., *Vestnik Moskov. Univ.* **8**, No. 9, *Ser. Fiz.-Mat. i Estestven. Nauk* No. 6, 109 (1953).
(4) Ingersoll, L. R., Zobel, O. J., Ingersoll, A. C., "Heat Conduction," McGraw-Hill, New York, 1948.
(5) Johnston, H. L., Grilly, E. R., *J. Chem. Phys.* **14**, 233 (1946).
(6) Kannuluik, W. G., Martin, L. H., *Proc. Roy. Soc. (London)* **A 144**, 496 (1934).
(7) Keyes, F. G., *Trans. Am. Soc. Mech. Engrs.* **73**, 589 (1951).
(8) *Ibid.*, **73**, 597 (1951).
(9) *Ibid.*, **74**, 1303 (1952).
(10) *Ibid.*, **76**, 809 (1954).
(11) Keyes, F. G., Sandell, D. J., Jr., *Ibid.*, **72**, 767 (1950).
(12) Lenoir, J. M., Junk, W. A., Comings, E. W., *Chem. Eng. Progr.* **49**, 539 (1953).
(13) Mason, H. L., *Trans. Am. Soc. Mech. Engrs.* **76**, 817 (1954).
(14) Meyers, C. H., *J. Research, Natl. Bur. Standards* **9**, 807 (1932).
(15) Reamer, H. H., Richter, G. N., Sage, B. H., *Ind. Eng. Chem.* **46**, 1471 (1954).
(16) Reamer, H. H., Sage, B. H., *Ibid.*, **44**, 185 (1952).
(17) Reamer, H. H., Sage, B. H., *Rev. Sci. Instr.* **24**, 362 (1953).
(18) Rothman, A. J., Bromley, L. A., *Ind. Eng. Chem.* **47**, 899 (1955)
(19) Sage, B. H., Lacey, W. N., *Trans. Am. Inst. Mining Met. Engrs.* **136**, 136 (1940).
(20) Sakiadis, B. C., Coates, Jesse, *A.I.Ch.E. Journal* **1**, 275 (1955).
(21) Schlinger, W. G., Sage, B. H., *Ind. Eng. Chem.* **42**, 2158 (1950).
(22) Sellschopp, W., *Forsch. Gebiete Ingenieurw.* **5B**, 162 (1934).
(23) Ubbink, J. B., de Haas, W. J., *Physica* **10**, 465 (1943).
(24) Vargaftik, N., *Tech. Phys. U.S.S.R.* **4**, No. 5, 341 (1937).

Received for review August 6, 1956. Accepted November 23, 1956.

This work was sponsored by Project SQUID which is supported by the Office of Naval Research under Contract N6-ori-105, T. O. III, NR-098-038. Reproduction in full or in part is permitted for any use of the United States Government.

Heat of Mixing of *n*-Amyl Alcohol and Benzene

DANIEL ALJURE CHALELA[1], HARRY H. STEINHAUSER, AND JOEL O. HOUGEN[2]
Rensselaer Polytechnic Institute, Troy, N.Y.

The objective of this work was to determine experimentally the heat of mixing of *n*-amyl alcohol in benzene over a range of compositions. Such information is useful in predicting thermodynamic properties of this binary mixture, particularly in connection with deviations from ideal behavior of vapor-liquid equilibrium relationships.

Because *n*-amyl alcohol in pure form tends to associate through hydrogen bonding to give linear polymers, its heat of mixing with an inert solvent, such as benzene, is endothermic. This corresponds to the rupture of hydrogen bonds during dilution.

Table I. Heat of Mixing of *n*-Amyl Alcohol in Benzene

Mole Fraction Benzene	ΔH^a of Mixing at 20° C., Cal./Gram Mole
0.158	91
0.260	126
0.325	183
0.331	177
0.473	214
0.483	219
0.485	213
0.497	212
0.650	223
0.758	208
0.837	177

[a] ΔH = enthalpy of mixture − enthalpy of pure components.

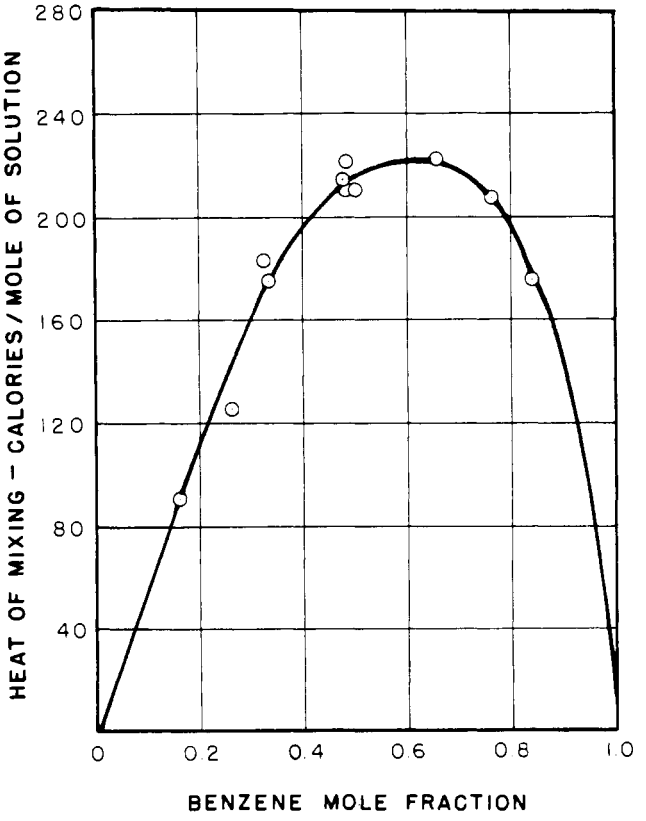

Figure 1. Heat of mixing of *n*-amyl alcohol in benzene

[1]Present address, National University, Bogota, Colombia, S.A.
[2]Present address, Research and Engineering Division, Monsanto Chemical Co., St. Louis, Mo.